Effect of ECAP on microstructure and mechanical properties of Cu-14Fe microcomposite alloy

2014 IOP Conf. Ser.: Mater. Sci. Eng. 63 012098

(http://iopscience.iop.org/1757-899X/63/1/012098)

Effect of ECAP on microstructure and mechanical properties of Cu-14Fe microcomposite alloy

N D Stepanov[a], A N Kozin[a], G A Salishchev[a] N E Khlebova[b], V I Pantsyrny[b]
[a]*Laboratory of Bulk Nanostructured Materials, Belgorod State University, 85 Pobeda Str., Belgorod, 803015, Russia*
[b]*LLC «Scientific Production Company «NANOELECTRO», Rogova 5A, Moscow, 123098, Russia*
E-mail: stepanov@bsu.edu.ru; stepanov.nikita@icloud.com

Abstract In current study the Cu-14%(wt.)Fe alloy was subjected to 1-10 ECAP passes via route A and, in addition, to 4 passes via routes Bc and C. Microstructure of the alloy after ECAP was characterized using SEM and EBSD analysis. It was shown that the refinement of Fe particles largely depended on the processing route: route A was the most efficient and route Bc was the less efficient. After 10 passes via route A the average thickness of Fe particles decreased to about 3 μm from about 10 μm in initial state. However, the microstructure development in Cu matrix was found to be not dependent much on ECAP route – the average grain/subgrain reached value of about 0.25 μm (according to EBSD analysis) after 4 passes. The mechanical properties of the alloy were also found to be not sensitive to ECAP routes. Ultimate tensile strength increased from 330 MPa in initial state to 545 MPa after 10 ECAP passes. Peculiarities of microstructural evolution of the alloy during ECAP as well as correlation between microstructure and mechanical properties are discussed.
Keywords: *Microcomposite alloy, ECAP, microstructure, mechanical properties.*

1. Introduction

During two recent decades huge attention was turned to refinement of structure of metallic materials by so called severe plastic deformation (SPD) [1] methods such as equal channel angular pressing (ECAP) [2] or high pressure torsion (HPT) [3]. Refining of structure down to ultrafine grained (UFG) level results in significant strengthening. However, it is known that refinement of structure and strengthening tends to saturate after moderate strains in most metals and alloys. For example, in case of ECAP saturation is observed already after 2-4 passes [4]. This problem could possibly be overcome in some alloys, such as so called microcomposite copper-based alloys [5]. These alloys are based on the systems with neglible solubility of the components at room temperature such as Cu-Nb, Cu-Ag, Cu-Fe etc, and usually contain ~10-30% of second component. Their microstructure consists from second component particles distributed in copper matrix. Plastic deformation usually introduced by conventional drawing or rolling, promotes continuous refinement of microstructure even at very high strains accompanied by strengthening [6, 7]. Such features make processing this kind of the alloys by SPD very attractive.

There is limited number of published papers on effect of SPD on microstructure and properties of microcomposite alloys. The most detailed studies were performed for Cu-Ag alloys, and were focused mainly on processing by high-pressure torsion (HPT) [8, 9]. HPT processing enables serious refinement of microstructure down to nanoscale level and increase of strength. But in terms of possible practical applications (it is well known that outstanding combination of strength and conductivity could by obtained in microcomposite alloys) relatively large-scale billets which could readily be produced by ECAP are of significant interest. But the data on feasibility of ECAP for refinement of microstructure of microcomposite alloys is rather ambiguous. In earliest research performed on Cu-Nb and Cu-Ag alloys possibility of significant strengthening was established [10]. More detailed studies on Cu-Ag alloys proved efficiency of ECAP in refinement of the structure [9, 11]; however, its efficiency was lower than of HPT [9]. It was also demonstrated that route A is the most effective route for producing fine microstructure and high strength [11]. However, no detailed studies are available for Cu-Fe alloys which are attractive for possible applications due to their relatively low cost. That is why the aim of current work is to study microstructure and mechanical properties of Cu-Fe alloy processed by ECAP using different routes and passes numbers.

2. Materials and methods

Ingot of Cu – 14.2(wt.)%Fe (further referred as Cu-14%Fe alloy) alloy was prepared by double vacuum arc remelting and cast into water-cooled copper mold. Initial ingot with diameter 105 mm was extruded to rod with diameter 45 mm. Extrusion was performed at 650 ˚C. Billets for ECAP (measuring 13.8 × 13.8 mm and length about 60 mm) were cut from extruded rod with electric discharge machine. Direction of pressing coincided with extrusion direction. ECAP was performed at room temperature; angle between channels was equal to 90°. MoS_2 grease was used for lubrication. ECAP was performed via route A (no rotation of billet between passes) with number of passes of 1, 2, 4 and 10. In addition, two billets were subjected to 4 ECAP passes via routes Bc (90°rotation) and C (180° rotation).

Microstructure of billets was characterized by scanning electron microscopy (Quanta 2003D both equipped with EDS detector). Microstructural characterization was carried out in three orthogonal sections, normal to extrusion direction (ED), transverse direction (TD) and normal direction (ND) correspondingly. Microstructure of Cu matrix was also studied utilizing electron backscattered diffraction (EBSD) technique. EBSD maps were obtained utilizing FEI Nova NanoSEM 450. Prior to analysis samples were carefully prepared by mechanically grinding and polishing the surface of the sample in a diluted OP-S solution. EBSD data was analyzed using OIM Analysis 6.0 software to produce inverse pole figure (IPF) maps. Standard cleanup procedure was used. High angle boundaries (HABs) with $\Theta \geq 15°$ are denoted with black lines on IPF maps, and low angle boundaries with $\Theta < 15°$ are denoted with white lines. Grain (i.e. crystallites limited by HABs) and subgrain (i.e. crystallites limited by LABs) size were calculated from IPF maps using standard linear interception method.

Tensile test was performed with an INSTRON 5882 testing machine at room temperature and initial strain rate of $1*10^{-3}s^{-1}$. Gauge dimensions of the specimens for tensile test were 16 mm in length, 3 mm in width and 1.5 mm in thickness.

3. Results

Microstructure of the as-cast and extruded alloy is shown on fig. 1a. Microstructure consists from Cu matrix with Fe particles inside. Fe particles appear almost equiaxed in ED section and are mostly elongated and aligned with extrusion direction in two other sections. However, microstructure in TD and ND sections is very inhomogeneous – individual Fe particles could be both nearly equiaxed or extremely oblong. EBSD map of Cu matrix of extruded alloy is given on fig. 1b. It is clearly seen that microstructure is mostly comprised from slightly elongated in extrusion direction subgrains with average size of about 0.57 µm. Fraction of HABs is as low as 22%, and HABs are mostly aligned with extrusion direction.

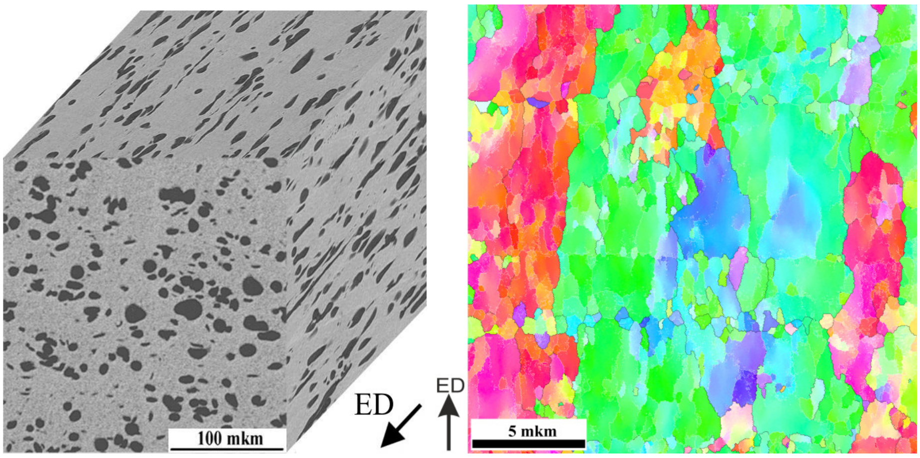

a b

Fig. 1. Microstructure of Cu-14Fe alloy in as-cast and extruded state: a – SEM-BSE image, 3 dimensional representation; b – EBSD-IPF map.

ECAP had not resulted in dramatic changes in microstructure as observed by SEM (fig 2). As the direction of extrusion after casting and direction of ECA pressing are the same, iron particles remained oriented in the same direction. The iron particles retain their mostly equiaxed form in ED section and are generally elongated in ND and TD sections. However, their shape evolved depending on both imposed strain and ECAP route. Effect of strain could be followed by comparison of microstructures of samples after 1, 2, 4 and 10 ECAP passes via A route (fig 2a, b, c, f). In ED section, after 1 pass (fig 2a) the particles became almost only round shaped. Further straining made shape of the particles more irregular, often very complex (fig 2b, c, f). This must be due to plastic deformation and fracture of individual particles. In ND and TD sections particles appeared similar and tent to become more elongated in extrusion direction with increase of processing strain. One should note that plastic deformation is very inhomogeneous, and together with deformed elongated particles nearly equiaxed particles remained even after large strains. Comparison between samples processed by 4 ECAP passes via different routes demonstrates that in average particles appeared more elongated after A (fig 2c) route and more equiaxed after Bc (fig 2a) route with route C being in-between two mentioned routes. The appearance of the particles in ND and TD sections also demonstrates that some of the particles are fractured during extrusion. They become exfoliated by copper streaks aligned in extrusion direction.

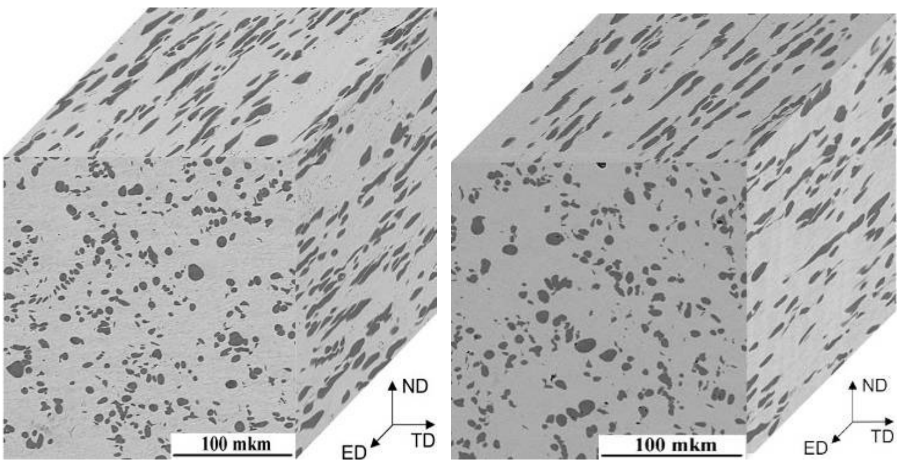

a b

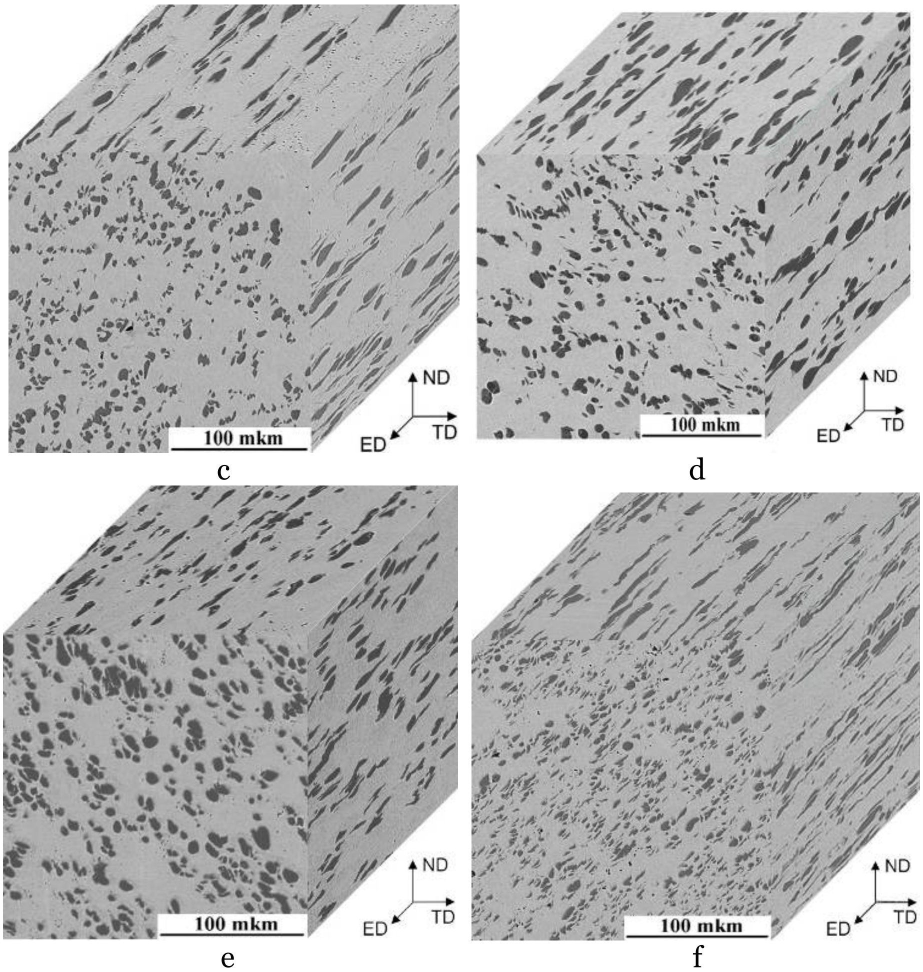

Fig. 2. Microstructure of the Cu-14%Fe alloy after ECAP, SEM-BSE images, 3 dimensional representation: a – 1 pass; b – 2 passes, route A; c – 4 passes, route A; d – 4 passes, route C, e – 4 passes, route Bc, f – 10 passes, route A.

Numerical information on dimensions of Fe particles is given in table 1. As in ED section particles appear quite equiaxed, the diameter of the particles was measured in this section. In two other sections, namely ND and TD, particles were elongated and thus both length and width of the particles was measured. Additionally spacing between the particles (in direction perpendicular to extrusion direction) in ND and TD sections was measured and also given in table 1. To illustrate effect of ECAP on microstructure further diameter of particles in ED section against passes number is plotted on figure 3a and spacing between particles in TD section against passes number is plotted on fig 3b. In initial extruded condition the average diameter of the particles in ED section was 10.2 µm, and average width of the particles in ND and TD sections was about 5.5-5.7 µm. The length of the particles in ND and TD sections was about 16.3-16.8 µm, and the average spacing between particles sections was of about 19.6-19.9 µm. It should be noted that no difference between dimensions of Fe particles in ND and TD sections were observed in initial state and this tendency remained the same after ECAP processing. After first ECAP pass substantial decrease of diameters of the Fe particles in ED section to 6.6 µm and increase of their length in ND and TD sections to 22.0-23.2 µm was observed. The spacing between the particles decreased to 16.2-16.4 µm. However, the width of the particles remained almost unchanged – 4.7-5.3 µm. After 2 passes via route A the diameter of the particles in ED section decreased further to 5.7 µm and length of the particles increased to 23.7-23.8 μm. Comparison of samples processed by 4 passes via different routes proves that A route is the most efficient for refinement of the particles and Bc route – the less efficient. For example, the average diameter of the particles in ED section was of 4.2 μm / 5.8 μm / 6.3 μm correspondingly for A / C / B_c routes (width of the particles in ND and TD sections demonstrated similar tendency), and length of the particles in ND and TD sections was of 25.0-25.5 μm / 20.8-23.0 μm / 16.5-16.7 respectively. Spacing between the particles also was lower after processing via A route (15.2 μm in TD section) than after C route (16.9 μm) and B_c route (17.4 μm). Finally, the thinnest (diameter of 3.1 μm in ED section) and the longest particles (length of 28.3-29.0 μm in ND and TD sections) with finest spacing between them of 13.5-13.8 μm were obtained after 10 ECAP passes via route A.

Table 1. Average Fe particle size in Cu-14%Fe alloy after ECAP.

Section	ED	ND			TD		
ECAP passes number and route	Diameter (μm)	Length (μm)	Width (μm)	Spacing (μm)	Length (μm)	Width (μm)	Spacing (μm)
0 (initial)	10.2±5.2	16.3±9.1	5.7±2.2	19.9±14.3	16.8±8.7	5.5±2.1	19.6±14.5
1	6.6±3.3	23.2±10.9	4.7±2.5	16.2±14.7	22.0±12.2	5.3±2.0	16.4±14.4
2 (A)	5.7±3.0	23.7±12.0	4.7±2.4	14.7±13.0	23.8±13.1	5.1±2.2	14.4±13.2
4 (A)	4.2±2.0	25.5±13.0	4.3±2.0	14.9±13.9	25.0±14.2	4.6±2.1	15.2±14.1
4 (C)	5.8±3.4	23.0±12.3	5.0±2.6	16.7±15.5	20.8±13.1	5.3±2.4	16.9±15.8
4 (Bc)	6.3±2.9	16.5±9.9	5.6±2.5	17.7±15.4	16.7±8.5	5.4±2.3	17.4±15.1
10 (A)	3.1±1.9	29.0±14.2	3.5±1.6	13.5±12.8	28.3±19.1	3.2±2.0	13.8±12.6

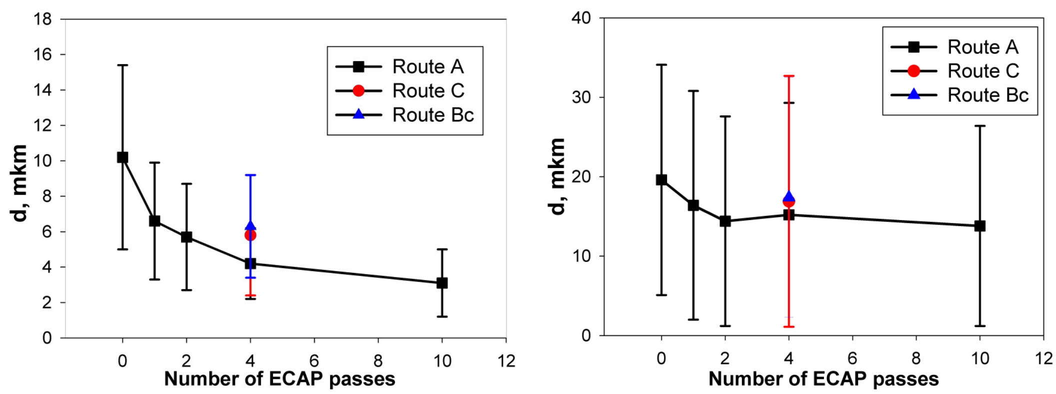

Fig. 3. Dependence of structural parameters of Cu-14%Fe alloy on number of passes: a- diameter of Fe particles in ED section; b – average spacing between Fe particles in TD section.

EBSD maps of Cu matrix of the Cu-14Fe alloy after ECAP are given in fig. 4. From fig 4a it is clearly seen that already after 1 ECAP pass microstructure of Cu matrix was significantly

IOP Conf. Series: Materials Science and Engineering **63** (2014) 012098 doi:10.1088/1757-899X/63/1/012098

refined in comparison with initial state (fig. 1b). Some equiaxed submicron grains appeared. However, the structure was very inhomogeneous and comprised mostly from large elongated in extrusion direction fragmented grains. Further straining to 2 passes via rote A (fig. 4b) resulted in formation of reasonably equiaxed microstructure. However, the microstructure was quite inhomogeneous and alongside with fine submicron grains many relatively coarse ones are observed. Comparison between samples processed by 4 ECAP passes via different routes demonstrates that most homogeneous and equiaxed structure is formed by utilization of B_c route (fig. 4e) with the microstructure after C route (fig. 4d) being comparable. The microstructure of the sample processed by A routes looks apparently less homogeneous. Even after 10 passes via route A (fig. 4e) the microstructure of Cu matrix remained quite inhomogeneous and was elongated in the extrusion direction.

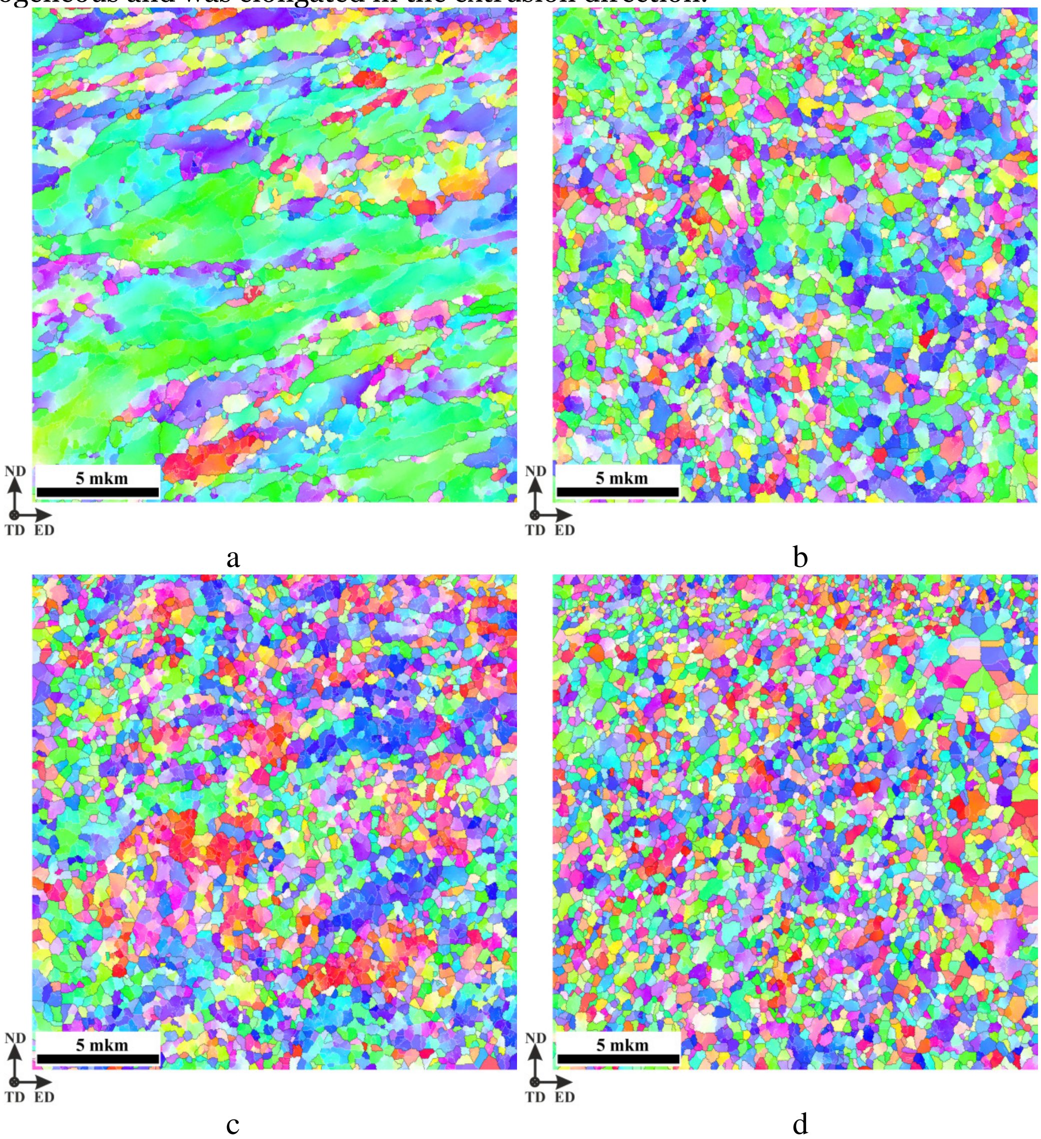

IOP Conf. Series: Materials Science and Engineering **63** (2014) 012098 doi:10.1088/1757-899X/63/1/012098

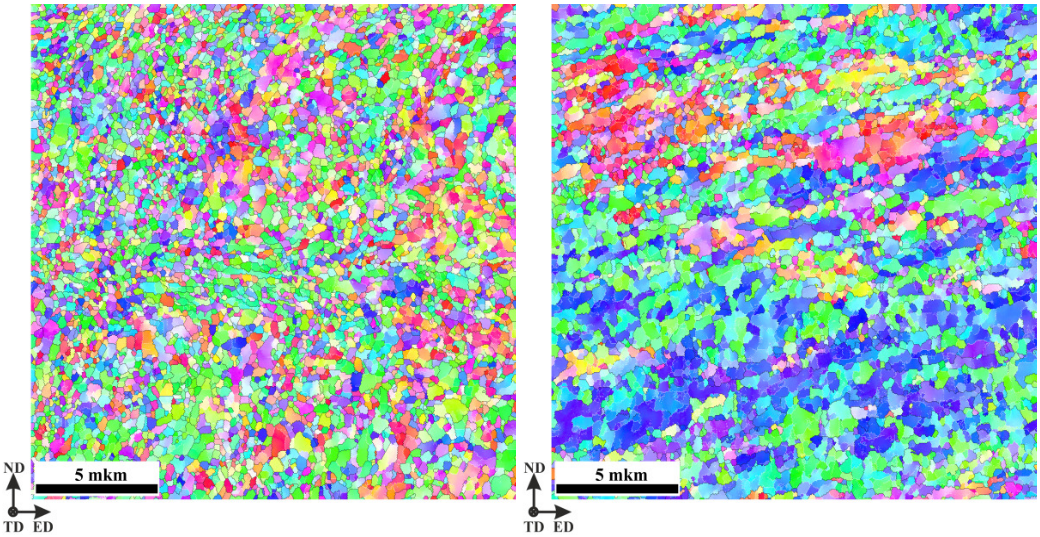

e f

Fig. 4. Microstructure of Cu matrix of the Cu-14%Fe alloy after ECAP, EBSD-IPF maps: a – 1 pass; b – 2 passes, route A; c – 4 passes, route A; d – 4 passes, route C, e – 4 passes, route Bc, f – 10 passes, route A.

Numerical data obtained by EBSD analysis such as average subgrain and grain average sizes and HABs fraction is summarized in Table 2. Already after the first ECAP pass significant structural refinement was obtained: the subgrain size decreases from 570 nm in initial state to 390 nm, grain size decreases from 880 nm to 530 nm and HABs fraction increases from 22% to 42%. Further plastic straining dopes not result in such pronounced refinement of microstructure of Cu matrix. After 2 ECAP passes via route A the average subgrain decreased to 330 nm, and after 10 passes it was of 260 nm. HABs fraction was of 58% and 52% respectively. Comparison between samples processed by 4 passes via different routes had demonstrated that subgrain size was almost identical for all routes – about 240-260 mn. But fraction of HABs was significantly higher after using B_c and C routes (73%) than after A route (53%). The average grain size was finer after B_c route (310 nm) than after C route (380 nm) and A route (430 nm).

Table 2. Average size of grains and subgrains and HABs fraction in Cu matrix of the Cu-14%Fe alloy after ECAP.

ECAP passes number and route	Average subgrain size, nm	Average grain size, nm	HABs fraction, %
0 (initial)	570±330	880±720	22
1	390±290	530±450	42
2 (A)	330±170	450±250	58
4 (A)	240±110	430±200	53
4 (Bc)	240±110	310±180	73
4 (C)	260±120	380±150	73
10 (A)	260±120	360±260	52

Stress-strain curves of the Cu-14Fe alloy in initial and ECAP-processed states are shown on fig. 5. Mechanical properties of the alloy in different states such as yield strength (Y.S.), ultimate tensile strength (U.T.S.), uniform elongation (ε_u) and elongation to fracture (ε_f) are summarized in Table 3. In initial (as-cast and extruded) state the alloy demonstrated relatively low strength, Y.S. equaled to 230 MPa and U.T.S. equaled to 330 MPa. The alloy was found to be ductile (ε_f=23%) and demonstrated high value of uniform elongation (ε_u=18%). The shape of stress-strain curve indicated significant capability of strain hardening. Mechanical properties were highly affected by ECAP. Already after first pass strength of the alloy substantially increased, Y.S. was equal to 405 MPa and U.T.S. was equal to 500 MPa. Strengthening was accompanied by rapid loss of plasticity, ε_u value decreased to 2.5% and ε_f value decreased to 8.2%. Further straining by 2 and 4 passes via route A has not resulted in substantial changes in mechanical properties, the yield strength values were of 413-415 MPa, and ultimate strength values were of 505-520 MPa. Uniform elongation values were of 2.1-2.2%, and elongation to fracture fluctuated from 8.9% to 13.0%.

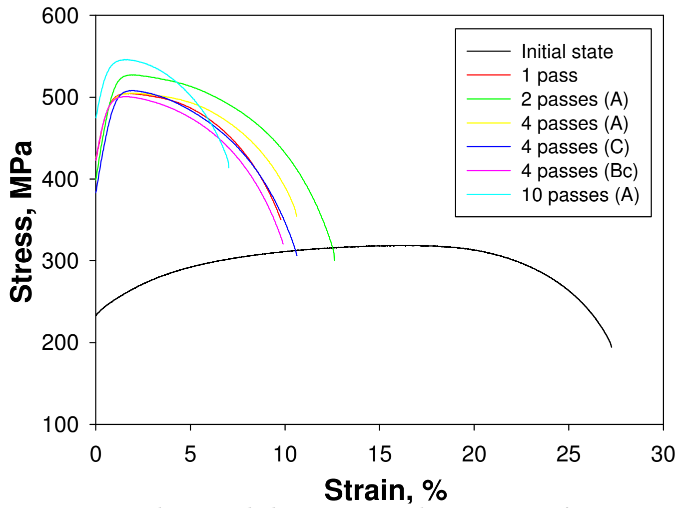

Fig. 5. Stress-strain curves obtained during tensile testing of Cu-14Fe alloy after ECAP.

Table 3. Mechanical properties of Cu-14Fe alloy after ECAP.

ECAP passes number and route	Y.S., MPa	U.T.S., MPa	ε_u,%	ε_f ,%
0 (initial)	230	330	18.0	23.0
1 (A)	405	500	2.5	8.2
2 (A)	413	520	2.1	13.0
4 (A)	415	505	2.2	8.9
4 (C)	432	505	2.4	12.0
4 (Bc)	442	508	1.5	10.0
10 (A)	425	545	1.7	7.2

Discussion

In current study, the microstructure and tensile properties of Cu-14Fe alloy in as-cast and extruded state and after ECAP with different number of passes and via different routes were examined. As the current alloy belongs to the family of so-called microcomposite alloys, it is possible to first discuss the structure of separate phases – Cu matrix and Fe particles – first, and their combineв effect on mechanical properties – at second.
The microstructure of the Cu matrix in initial (as-cast and extruded) condition in accordance with EBSD analysys consisted mainly from subgrains (HABs fraction of 22%) with average size of about 570 nm, which correlates well with results our earlier TEM studies [12] that revealed presence of grains/subgrains with average size of 500 nm. ECAP results in pronounced decrease of grain/subgrain size and increase of HABs fraction. It should be noted that the obtained values of grain/subrain size (240-260 nm after 4-10 passes) and HABs fraction (52-72% after 2-10 passes) after ECAP are in good agreement with the data reported for pure copper processed by ECAP [13-15]. Also, overall trends – saturation of structural refinement after first several passes [15], higher efficiency of Bc route in comparison with A route in producing homogenious equiaxed structure with high fraction of HABs [2] are similar to those found for pure materials processed by ECAP. So one can state that microstructure of Cu matrix of the Cu-14Fe alloy after ECAP is reasonably close to those of pure copper after similar processing.
The morphology of the Fe particles which were mostly elongated in extrusion direction in initial state evolves slightly during ECAP. They become more aligned with extrusion direction. This is mirrored in the fact that value of particles diameter in ED section, which was about two times higher than their thickness in ND and TD direction in initial condition (table 1), becomes equal to the thickness of the particles after 4 and 10 ECAP passes. Also, one might state that the rapid decrease of diameter of the particles in ED section (fig. 3a) is mostly related with alignment of the particles with extrusion direction as thickness of the particles in ND and TD sections decreased much less. Plastic deformation introduced during ECAP results in refinement of the particles. They become both thinner and longer after pressing than they were in initial state, after 10 passes the difference of particle dimensions with those for initial state is about two times. That implies that particles are "stretched" in extrusion direction during pressing. The effect of "stretching" largely depends on route, as it could be seen from the comparison of microstructure of the samples processed by 4 passes (fig 2 c-e, table 1). Higher efficiency of A route is quite anticipated as it involves continuous stretching of the particles in one constant direction, whereas other routes involve constant change in shear direction and thus are not that effective. Higher efficiency of route A in comparison with routes C and especially Bc was also found for Cu-8Ag alloy [11]. Fe particles do not only plastically deform during ECAP, but also undergo fracture, as it may be seen from SEM images (fig. 2). Most probably fracture of particles is related with development of lamination process, previously observed in the same Cu-14Fe alloy during rolling [12]. This process should be the main contributor to the continuous decrease of the spacing between the particles observed during ECAP (table 1, fig. 3b). However, the decrease of spacing between the particles after ECAP is not very pronounced even after 10 passes – the corresponding values decreases from about 20 μm to 13.5-13.8 μm.
The spacing between the particles of the second component (Fe in case of Cu-14Fe alloy) is thought to be crucial parameter in microcomposite alloys as in many cases Hall-Petch type dependence between strength of the alloy and spacing between the particles is found [12, 16, 17]. For the studied alloy Hall-Petch type dependence of U.T.S. of particle spacing was found after rolling [12]. However, values of U.T.S. plotted against particle spacing on fig. 6 demonstrate almost no correlation between strength and spacing between particles. It is clearly seen that after ECAP, despite the continuous decrease of particle spacing, the strength

remains on the same level. This means that Hall-Petch type relationship could not be used to explain strengthening of the Cu-14Fe alloy during ECAP.

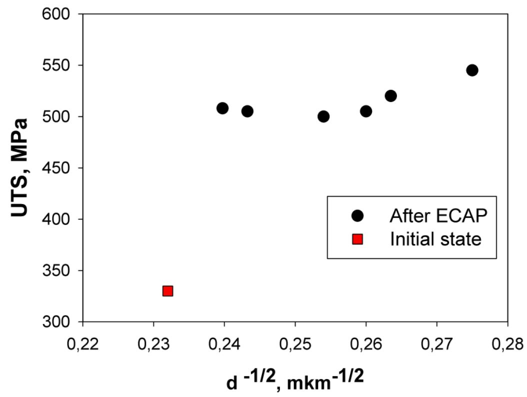

Fig. 6. Dependence of ultimate tensile strength (UTS) on distance between Fe particles.

In most cases, strength of composite materials is determined by rule of mixtures (ROM), which means that strength of overall material is equal to sum of strength of its components multiplied on their volume fraction. For drawn microcomposite Cu-20Fe alloy it was shown that specific value of particle spacing has to be achieved to obtain Hall-Petch behavior [17]. In that work, critical value of 6.5 μm was determined. In our case, even minimal values of particle spacing after 10 passes are about two times higher than the critical value of 6.5 μm, thus ROM should be used to explain mechanical properties of the alloy. One should also note that efficiency of strengthening by the particles is dependent on their morphology [16], and ellipsoidal particles observed after ECAP are expected to much less effective than complexly curved particles after drawing. So for ECAP processed microcomposite alloys the critical value for transition to Hall-Petch strengthening could be even higher that for drawn alloys.

Indirect prove of validity of ROM in case of structure-properties relationship of ECAP-processed could be found in the fact that the overall dependence of mechanical properties on number of passes is very similar to those for pure metals, especially copper. Mechanical properties of pure copper after ECAP were assessed in a number of papers [14, 15]. It is well accepted that substantial increase of strength is observed only after first few passes, and after that only slight fluctuations of strength are possible. As copper is the matrix phase of the Cu-14Fe alloy with volume fraction of 84%, there is no surprise that the whole alloy demonstrates very similar behavior – pronounced strengthening after first pass and almost constant level of strength after further processing. More precisely, validity of ROM could be tested by comparison the experimentally observed values with calculated from ROM. Strength of the individual phases could be found in literature. Here we have used the values of 395 MPa for U.T.S. of pure copper (after 4 ECAP passes via route B_c [15]) and 1030 MPa for U.T.S. of pure iron (Armco iron, processed by 7 passes with channel interception angle of 120° which gives the imposed strain equal to 4 passes with interception angle of 90°C via route A [18]), and the volume fractions respectively of 84% and 16%. The calculations have returned U.T.S. value of 475 MPa, which is very close to experimentally observed 505-508 MPa, observed after 4 passes via different routes. Good correspondence between experimental values and calculated one indicates that ROM could be successfully used to predict strength of Cu-14Fe alloy processed by ECAP.

Conclusions

1) ECAP results in refinement of microstructure of the Cu-14Fe alloy. UFG structure with average grain/subgrain size of about 250 nm and fraction of HABs higher than

50% is formed in Cu matrix after 4 and more ECAP passes. Fe particles become stretched in extrusion direction after ECAP, their thickness decreases to 3.2-3.5 μm after 10 passes. The distance between the Fe particles also decreases to 13.5-13.8 μm after 10 ECAP passes.

2) Significant strengthening of the Cu-14Fe alloy is observed as the result of ECAP processing. Ultimate tensile strength is increased to 500 MPa already after 1 pass. Further increasing of number of passes results only in slight increase of strength. Tensile ductility is decreased to about 10% as the result of ECAP processing. It is shown that strength of the Cu-14Fe follows the rule of mixtures.

References

[1] R. Z. Valiev, Y. Estrin, Z. Horita, T. G. Langdon, M. J. Zehetbauer and Y. T. Zhu: Min. JOM - J, Met. Mater. Soc. Vol. **58** (2006) pp. 33–39.
[2] R.Z. Valiev, T.G. Langdon: Prog. Mater. Sci. Vol. **51** (2006) pp. 881-981.
[3] A.P. Zhilyaev, T.G. Langdon: Prog. Mater. Sci. Vol. **53** (2008), pp. 893-979.
[4] R. Pippan, S. Scheriau, A. Taylor, M. Hafok, A. Hohenwarter, A. Bachmaier: Ann. Rev. Mat. Res. Vol. **40** (2010) pp. 319-343.
[5] F. Heringhaus, D. Raabe: J. Mater. Process. Tech. Vol. **59** (1996) pp. 367-372.
[6] Y.S. Go, W.A. Spitzig: J. Mater. Sci. Vol. **26** (1991) pp. 163 – 171.
[7] G.A. Jerman, I.E. Anderson, J.D. Verhoeven: Metall. Trans. A Vol. **24** (1993) pp. 35-42.
[8] Y.Z. Tian, S.D. Wu, Z.F. Zhang, R.B. Figueiredo, N. Gao, T.G. Langdon: Acta Mater. Vol. **53** (2011) pp. 2783-2796.
[9] Y.Z. Tian, S.D. Wu, Z.F. Zhang, R.B. Figueiredo, N. Gao, T.G. Langdon: Mater. Sci. Eng. Vol. **528** (2011) pp. 4331-4336.
[10] V.M. Segal, W.T. Hartwig, R.E. Goforth: Mater. Sci. Eng. Vol. **224** (1997) pp. 107-115.
[11] Y.Z. Tian, Q.Q. Duan, H.J. Yang, H.F. Zou, G. Yang, S.D. Wu, Z.F. Zhang: Metall. Mater. Trans. Vol. **41A** (2010) pp. 2290-2303.
[12] N.D. Stepanov, A.V. Kuznetsov, G.A. Salishchev, N.E. Khlebova, V.I. Pantsyrny: Mater. Sci. Eng. A Vol. **264** (2013) pp. 264-272.
[13] F.H. Dalla Torre, A.A. Gadzer et al: J. Mater. Sci. **42** (2007) pp. 9097-9111.
[14] F.H. Dalla Torre, A.A. Gadzer et al: Metall. Mater. Trans. **A 38** (2007) pp. 1080-1095.
[15] N.D. Stepanov, A.V. Kuznetsov, G.A. Salishchev, G.I. Raab, R.Z.Valiev: Mater. Sci. Eng. A Vol. **254** (2012) pp. 105-115.
[16] W.A. Spitzig: Scripta Metall. Vol. **23** (1989) pp. 1177-1180.
[17] Y.S. Go, W.A. Spitzig: J. Mater. Sci. Vol. **26** (1991) pp. 163-171.
[18] A. Hohenwarter, R. Pippan: Acta Mater. Vol.**61** (2013) pp. 2973-2983.